RATE-OPTIMAL SIGNAL DESIGN FOR WIRELESS COMMUNICATIONS

Saswat Misra* and Ananthram Swami
Army Research Laboratory
Adelphi, MD, USA

Lang Tong
Cornell University
Ithaca, NY, USA

ABSTRACT

In a tactical communications scenario, the transmitter will only have an imperfect estimate of the temporally correlated mobile RF channel. Given imperfect channel state information (CSI), we address the optimal signal design problem. Using the cutoff rate metric, we determine: (a) the optimal allocation of power and bandwidth between information and training signals, (b) the optimal binary input as a function of SNR and CSI quality, (c) an adaptive modulation scheme which switches between only two inputs based on the CSI quality. We show that this simple adaptive modulation scheme is nearly optimal at moderate to high SNR. We also establish that there is at most a 1 dB increase in the maximum penalty for using On-Off Keying instead of BPSK.

1. INTRODUCTION

Future military communication systems will be deployed in rapidly changing, mobile battlefield scenarios [2]. Communications in these settings will be severely energy-limited, and hostile channel conditions will be encountered. Inefficient energy usage leads to compromised LPD/LPI features; it increases the interference to other blue radios, reduces network lifetime, and increase the size and weight of batteries, thereby negatively impacting the Objective Force Warrior.

Optimized energy allocation and adaptive modulation schemes can be used, and these techniques often result in significant energy savings [4]. However, they require knowledge of the communications channel at the transmitter and receiver. The receiver typically obtains this channel state information (CSI) by using a standard estimation algorithm, and ideally, feeds this information back to the transmitter. However, if the channel is rapidly time-varying, then estimates become will become outdated by the time they reach the transmitter, and this makes feedback impractical (feedback may also be difficult or severely limited in many other scenarios of interest). Alternatively, there are many cases where the transmitter has some statistical knowledge of the mobility scenarios and the channel estimation algorithms used by the receiver. In this case, it can statistically predict the quality of the channel estimates, and as a result, it can adapt its energy allocation and modulation schemes accordingly, without any explicit feedback.

We model the channel as a single-user Rayleigh fading channel with temporal correlation, and use the channel cutoff rate [8] to design the optimal signaling strategy for the described scenario. The cutoff rate is a well known information theoretic metric, and has been frequently used to characterize the bit error rate, achievable information rates, and decoding complexity of coded transmission over wireless fading channels [4]. Cutoff rate has also been called the 'computational capacity', in the context of sequential decoding. It has been studied under the assumptions of no CSI (" blind") in [6] and full CSI ("known channel") in [7].

In Section 2 we introduce the channel model, and a pilot-symbol assisted modulation (PSAM) channel estimation scheme. We then find the cutoff rate for this front-end under binary signaling. In Section 3 we derive the optimal power allocation between training and information symbols, and provide a bound on the optimal bandwidth allocation. In Section 4, we analyze the rate-optimal binary input as a function of the SNR and CSI quality available at the receiver. We study the limiting optimal distributions, BPSK and On-Off Keying (OOK), and find an analytic design rule that allows adaptive modulation as the receiver CSI degrades. We show that switching between just BPSK and equiprobable-OOK achieves nearly optimal binary signaling for moderate (≈ 0 dB) to large SNR, and that switching between just BPSK and the OOK family of distributions is nearly optimal for all SNR. In Section 5, we derive the energy required to achieve a target cutoff rate. For an AWGN channel, we know that OOK suffers from a 3dB penalty over BPSK. We show that for the case of a fading channel, and partial CSI, the penalty is in the range $(-\infty, 4)$ dB (a negative penalty denotes a "gain"). We asses the benefits of generalized OOK and show that, while the 3 dB penalty can be fully recovered at small rates, with an additional energy

Report Documentation Page

Form Approved
OMB No. 0704-0188

Public reporting burden for the collection of information is estimated to average 1 hour per response, including the time for reviewing instructions, searching existing data sources, gathering and maintaining the data needed, and completing and reviewing the collection of information. Send comments regarding this burden estimate or any other aspect of this collection of information, including suggestions for reducing this burden, to Washington Headquarters Services, Directorate for Information Operations and Reports, 1215 Jefferson Davis Highway, Suite 1204, Arlington VA 22202-4302. Respondents should be aware that notwithstanding any other provision of law, no person shall be subject to a penalty for failing to comply with a collection of information if it does not display a currently valid OMB control number.

1. REPORT DATE	2. REPORT TYPE	3. DATES COVERED
00 DEC 2004	**N/A**	**-**

4. TITLE AND SUBTITLE	5a. CONTRACT NUMBER
Rate-Optimal Signal Design For Wireless Communications	5b. GRANT NUMBER
	5c. PROGRAM ELEMENT NUMBER
6. AUTHOR(S)	5d. PROJECT NUMBER
	5e. TASK NUMBER
	5f. WORK UNIT NUMBER
7. PERFORMING ORGANIZATION NAME(S) AND ADDRESS(ES) **Army Research Laboratory Adelphi, MD, USA; Cornell University Ithaca, NY, USA**	8. PERFORMING ORGANIZATION REPORT NUMBER
9. SPONSORING/MONITORING AGENCY NAME(S) AND ADDRESS(ES)	10. SPONSOR/MONITOR'S ACRONYM(S)
	11. SPONSOR/MONITOR'S REPORT NUMBER(S)

12. DISTRIBUTION/AVAILABILITY STATEMENT
Approved for public release, distribution unlimited

13. SUPPLEMENTARY NOTES
See also ADM001736, Proceedings for the Army Science Conference (24th) Held on 29 November - 2 December 2004 in Orlando, Florida., The original document contains color images.

14. ABSTRACT

15. SUBJECT TERMS

16. SECURITY CLASSIFICATION OF:			17. LIMITATION OF ABSTRACT	18. NUMBER OF PAGES	19a. NAME OF RESPONSIBLE PERSON
a. REPORT	b. ABSTRACT	c. THIS PAGE			
unclassified	**unclassified**	**unclassified**	**UU**	**8**	

savings if the CSI quality exceeds a threshold, this penalty cannot be improved at large rates.

We use the following notation and definitions: (a) $x \sim \mathcal{CN}\left(\mu, \sigma^2\right)$ is a complex Gaussian random variable x with mean μ and with independent real and imaginary parts, each having variance $\sigma^2/2$, (b) $\mathcal{E}[.]$ is the expectation operator, (c) superscripts "t", and "c" denote transposition, and complex conjugation, and (d) $[k] \triangleq k \mod T$, where T is an integer.

2. SYSTEM MODEL

We introduce the channel model and estimation scheme, and review the cutoff rate metric.

2.1. Channel Model

In the standard Rayleigh fading time-correlated model, the received signal is

$$y'_k = \sqrt{E_k} h'_k s_k + n'_k,$$

where s_k is the input, and $n'_k \sim \mathcal{CN}\left(0, \sigma_N^2\right)$ describes AWGN. The transmission energy used at time k is $E_k|s_k|^2$, and $h'_k \sim \mathcal{CN}\left(0, \sigma_h^2\right)$ denotes the fading process and has correlation function $R_h(\tau) \triangleq \frac{1}{\sigma_h^2}\mathcal{E}\left[h'_k h'^c_{k+\tau}\right]$.

We assume that training is sent periodically once every T transmissions, at times $k = mT$. At each time $mT + \ell$ $(0 \le \ell \le T-1)$, a minimum mean square error (MMSE) estimate of the channel $\widehat{h}'_{mT+\ell}$ is made at the receiver using some subset $\mathcal{N}$ of past and future training symbol observations, so that $\widehat{h}'_{mT+\ell} = \mathcal{E}[h'_{mT+\ell}|\{y'_{nT}\},\ n \in \mathcal{N} \subset \mathcal{Z}]$. The use of an MMSE estimator implies that $\widehat{h}'_{mT+\ell} \sim \mathcal{CN}\left(0, \widehat{\sigma}_\ell^2\right)$ and that the estimation error $\widetilde{h}'_{mT+\ell} \sim \mathcal{CN}\left(0, \sigma_h^2 - \widehat{\sigma}_\ell^2\right)$. Thus, $\widehat{h}'_{mT+\ell}$ and $\widetilde{h}'_{mT+\ell}$ are independent. To characterize the performance of a particular estimator, we will define the *estimator quality* as

$$\omega_\ell \triangleq \widehat{\sigma}_\ell^2/\sigma_h^2.$$

Note that $0 \le \omega_\ell \le 1$. We will find it useful to define the *received SNR*

$$\kappa_\ell \triangleq \sigma_h^2 E_\ell/\sigma_N^2.$$

The system equation becomes

$$y'_k = \sqrt{E_{[k]}} h'_k s_k + n'_k = \sqrt{E_{[k]}}\left(\widehat{h}'_k + \widetilde{h}'_k\right) s_k + n'_k,$$

where, given the periodic nature of the training, we have assumed that the energy allocation is also periodic. For binary signalling, we can assume that the signal set (but not the channel) is real valued; The input s_k is selected from signal set $\mathcal{S}_{[k]} = \{A_{[k]}, -B_{[k]}\}$ and subject to a unit average-energy constraint: $p_{[k]}A_{[k]}^2 + (1-p_{[k]})B_{[k]}^2 = 1$, where $p_{[k]}$ is the probability of transmitting $A_{[k]}$. In the training slots ($k = mT$), we let $s_k = +1$ (i.e., $\mathcal{S}_0 = \{+1\}$).

We assume that perfect interleaving is performed at the transmitter [3], and that channel estimation is performed before deinterleaving at the receiver. The effective *system equation* is then

$$y_k = \sqrt{E_{[k]}} h_k s_k + n_k = \sqrt{E_{[k]}}\left(\widehat{h}_k + \widetilde{h}_k\right) s_k + n_k,$$

where $h_k \sim \mathcal{CN}\left(0, \sigma_h^2\right)$ and $n_k \sim \mathcal{CN}\left(0, \sigma_N^2\right)$ are i.i.d. sequences representing the interleaved channel and noise sequences. Interleaving implies that $\widehat{h}_k$ and $\widetilde{h}_k$ are independent sequences in k, and also with respect to each other. Interleaving preserves the marginal statistics of the channel estimate and estimation error: $\widehat{h}_{mT+\ell} \sim \mathcal{CN}\left(0, \widehat{\sigma}_\ell^2\right), \widetilde{h}_{mT+\ell} \sim \mathcal{CN}\left(0, \sigma_h^2 - \widehat{\sigma}_\ell^2\right)$, and $\widehat{h}_{mT+\ell}$ and $\widetilde{h}_{mT+\ell}$ are independent. Finally, we assume that codewords are decoded using the ML-detector which treats $s_{mT+\ell}$ as the channel input and the pair $(y_{mT+\ell}, \widehat{h}_{mT+\ell})$ as the channel output.

2.2. Cutoff Rate

We now derive the cutoff rate for the system front-end described in Section 2. The cutoff rate is [8]

$$R_o = -\min_{Q(.)} \frac{1}{T}\log_2 \int_{\mathbf{y}} \left[\sum_{\mathbf{s}} Q(\mathbf{s})\sqrt{P(\mathbf{y}, \widehat{\mathbf{h}} \mid \mathbf{s})}\right]^2 d\mathbf{y},$$

where $\widehat{\mathbf{h}} \triangleq \left[\widehat{h}_{mT+1}, \ldots, \widehat{h}_{(m+1)T-1}\right]^t$ is the estimated channel, $\mathbf{y} \triangleq \left[y_{mT+1}, \ldots, y_{(m+1)T-1}\right]^t$ the observation, and $\mathbf{s} \triangleq \left[s_{mT+1}, \ldots, s_{(m+1)T-1}\right]^t$ the signal corresponding to the m^{th} T-length "super-symbol." The input distribution $Q(\mathbf{s}) = \prod_{\ell=1}^{T-1} Q_\ell(s_{mT+\ell})$, where $Q_k(A_k) = p_k$ and $Q_k(B_k) = 1 - p_k$.

In [9] we evaluated this expression for the system front-end described, and found that $R_o =$

$$-\frac{1}{T}\sum_{\ell=1}^{T-1} \min_{\mathcal{C}(p_\ell, A_\ell, B_\ell)} \log_2\left[1 + 2p_\ell\left(1-p_\ell\right)\left(\Gamma_\ell - 1\right)\right], \quad (1)$$

where $\mathcal{C}(p, A, B) \triangleq \{(p, A, B) : 0 \le p \le 1,\ 1 \le A < \infty,\ 0 \le B \le 1,\ pA^2 + (1-p)B^2 = 1\}$ is the constraint set, and where

$$\Gamma_\ell \triangleq \frac{\sqrt{1 + \kappa_\ell\left(1-\omega_\ell\right)|A_\ell|^2}\sqrt{1 + \kappa_\ell\left(1-\omega_\ell\right)|B_\ell|^2}}{1 + \frac{\kappa_\ell}{2}\left(1 - \frac{\omega_\ell}{2}\right)\left(|A_\ell|^2 + |B_\ell|^2\right) + \frac{\kappa_\ell\omega_\ell}{2}|A_\ell - B_\ell|^2}.$$

Each term in the sum above represents the cutoff rate in one data "channel", given as a function of ω_ℓ and κ_ℓ. In the remaining sections, we consider the energy allocation and modulation types that maximize the rate R_o, as well as the energy penalty for using suboptimal strategies.

3. OPTIMAL TRAINING

We consider the optimal energy allocation and the optimal training period for the PSAM estimation scheme described in Section 2. Here, we consider BPSK ($p_\ell = \frac{1}{2}, A_\ell = -B_\ell = 1$),for which the cutoff rate becomes

$$R_o = -\frac{1}{T}\sum_{\ell=1}^{T-1}\log_2\left\{1 - \frac{\omega_\ell}{2}\frac{\kappa_\ell}{1+\kappa_\ell}\right\}.$$

For simplicity, we restrict the analysis to causal estimators ($\max\mathcal{N} \leq m$). However, many of the following results can be extended to non-causal estimators as well, see [10].

3.1. Energy Allocation

We impose an average energy constraint $\kappa_0 + (T-1)\kappa_1 \leq \kappa_{\text{av}}T \triangleq \kappa_{\text{tot}}$, and seek the optimal energy distribution (κ_0^*, κ_1^*) between training and data, which is given implicitly in the following:

R1. For any causal estimator $(\max\{\mathcal{N}\} \leq m)$ with estimator quality ω_ℓ, κ_0^* is given implicitly in terms of the estimation quality in the pilot slot ω_0 as follows:

$$\kappa_0^* = \arg\max_{0\leq\kappa_0\leq\kappa_{\text{av}}\,T}\left[\frac{\kappa_{\text{av}}T-\kappa_0}{\kappa_{\text{av}}T-\kappa_0+(T-1)}\ \ \omega_0\right].$$

We state a corollary of the above result:

C1. For the "last-pilot" estimator, $(\mathcal{N} = m)$, the optimal data energy is independent of $R_h(\tau)$, and is

$$\kappa_1^* = \Gamma - \sqrt{\Gamma^2 - \frac{\kappa_{\text{av}}T}{T-1}\Gamma},\ \ \Gamma = \frac{\kappa_{\text{av}}T+1}{T-2}.$$

for $T > 2$. For $T = 2$, $\kappa_1^* = \kappa_0^* = \kappa_{\text{av}}$. In the high-SNR scenario ($\kappa_{\text{tot}} \to \infty$), we find that $\kappa_0^* = \kappa_{\text{av}}T\left[\frac{\sqrt{T-1}-1}{T-2}\right]$. For large T, the energy allocated to the training symbol increases as $\kappa_{\text{av}}\sqrt{T}$. For low-SNR ($\kappa_{\text{av}} \to 0$), we find that $\kappa_0^* = (\kappa_{\text{av}}/2)T$, i.e., half of the available energy should be allocated to the pilot symbol. More generally, we find that:

R2. At low-SNR, $\kappa_0^* = \kappa_{\text{tot}}/2$ for any estimator $\mathcal{N}$, i.e., half of the available energy should be allocated to training.

3.2. Training Period

The energy allocation strategy above is for a fixed training period T. Here, we seek the optimal training period. We derived the following result in [10]:

R3. Assume that $R_h(\tau)$ is monotonically decreasing over $T \in [0, T_{\max}]$. For any casual estimator, a lower bound on the optimal training period in the range, $[0, T_{\max}]$, is given by the high-SNR scenario. Furthermore, the bound is exact at high-SNR, is the same for all casual estimators, depends only on $R_h(\tau)$, and is given by

$$T_B = \arg\min_T \prod_{\ell=1}^{T-1}\left[1 - \frac{R_h^2(p\,T+\ell)}{2}\right]^{1/T},$$

where $p \triangleq m - \max\{n \in \mathcal{N}\}$ is the number of pilots between the most recent pilot and the last pilot used.

The bound is compared to the optimal value of the training period in Table 1. We consider two channel models, an AR-1 model for which $R_h(\tau) = \alpha^{|\tau|}, 0 < \alpha < 1$, and the Jakes model for which $R_h(\tau) = J_o(2\pi f_D T_D \tau)$, where $f_D T_D$ is the normalized Doppler. The first column is the average energy per slot, the second and third columns are the optimal training periods using the last pilot $(1,0)$ and the infinite past $(\infty,0)$ for the AR-1 model. The fourth column is the bound computed according to result R3. Similarly, the fifth and sixth columns show the optimal training period and bound for the Jakes model, for the last-pilot estimator. Note that the bound is tight, particular at moderate-to-high SNR's. An extension of these results to non-casual estimators is given in [10].

κ_{av}	$T^{\text{AR-1}}_{(1,0)}$	$T^{\text{AR-1}}_{(\infty,0)}$	$T^{\text{AR-1}}_{B}$	$T^{\text{Jakes}}_{(1,0)}$	T^{Jakes}_{B}
$\alpha = \mathbf{0.95}$				$f_DT_D = \mathbf{0.25}$	
1	8	5	**5**	7	**5**
10	5	5	**5**	5	**5**
100	5	5	**5**	5	**5**
$\alpha = \mathbf{0.99}$				$f_DT_D = \mathbf{0.01}$	
1	20	11	**9**	14	**9**
10	11	10	**9**	10	**9**
100	9	9	**9**	9	**9**

Table 1. Illustration of the training period bound.

4. RATE-OPTIMAL MODULATION

Here we answer the question: What is the optimal binary modulation scheme for each slot? From the cutoff rate expression in (1), the optimal binary input in the ℓ^{th} channel is independent of ℓ, in that it depends only on the CSI quality ω and SNR κ in that channel. Therefore, we drop the ℓ subscript, and seek (p^*, A^*, B^*), from

$$\min_{\mathcal{C}(p,A,B)} p\,(1-p)\left\{\frac{\sqrt{1+\kappa\,(1-\omega)\,A^2}\sqrt{1+\kappa\,(1-\omega)\,B^2}}{1+\frac{\kappa}{2}\ (1-\frac{\omega}{2})\,(A^2+B^2)+\frac{\kappa\,\omega}{2}AB} - 1\right\}. \tag{2}$$

The behavior of the optimal binary input is shown in Figure 1, parameterized by ω. Next, define the positive root of the polynomial $3\omega^2 - 6\omega + 2$ as $\omega^* \triangleq 1 - 1/\sqrt{3}$. Then the overall behavior is described by the following remarks (for proofs and further discussion, see [9]):

R4. *For small SNR ($\kappa << 1$)*: . If $\omega < \omega^*$, then A^* decreases as ω increases. Correspondingly, p^* and B^* are increasing in ω. As $\kappa \to 0$, $A^* \to \infty$ and $p^* \to 0$

such that $pA^2 \to 1$. That is, as $\kappa \to 0$, $\lim_{p\to 0} \text{OOK}(p)$ is optimal.[1] If $\omega \geq \omega^*$, the optimal binary distribution is the BPSK solution, $A = B = 1, p = 1/2$.

R5. *For large SNR ($\kappa >> 1$):* If $\omega < \omega^*$, then from Figure 1, A^* decreases with SNR. If $\omega > \omega^*$, A^* increases with SNR, reaches a peak, and then decreases monotonically to $\sqrt{2}$. As SNR $\to \infty$, OOK$(1/2)$ is optimal for $\omega \neq 1$. That OOK$(\frac{1}{2})$ is cutoff rate-optimal at high SNR when $\omega = 0$ is not surprising given the capacity analysis of [1]. However, we find it interesting that this input remains cutoff rate-optimal for *any* $\omega \neq 1$ at high SNR.

R6. *The probability of transmitting A, p, satisfies* $p \leq 1/2$.

Having examined the general behavior of the optimal input, we will now focus on the two limiting cases of no CSI ($\omega = 0$) and full CSI ($\omega = 1$).

4.1. Cutoff Rate for BPSK

First, we consider the case where full CSI is available at the receiver. Letting $\omega = 1$ in (2), we find that the maximum occurs at $A = B,$ and $p = 1/2$, implying that BPSK modulation maximizes the cutoff rate. For arbitrary ω, the cutoff rate for BPSK is given by

$$R_{o,B} = -\log_2 \left\{ 1 - \frac{\omega}{2} \frac{\kappa}{1+\kappa} \right\}. \tag{3}$$

We make the following observations:

R7. At high SNR, $\kappa/(1+\kappa) \to 1$. Therefore, the CSI quality places an asymptotic ceiling on the cutoff rate $R_{o,B}$

R8. When $\omega = 0$ (no CSI is available), information transmission is not possible. This is because the statistics of y_k at the receiver are independent of s_k; i.e.,

$$y_k | s_k \ \sim \ \mathcal{CN}\left(0,\ \sigma_N^2(1+\kappa)\right).$$

R9. More generally, the statistics of y_k under the two hypotheses, and conditioned upon the known part of the channel $\widehat{h}_k$, are

$$y_k | \widehat{h}_k, s_k \ \sim \ \mathcal{CN}\left(\sqrt{E}\,\widehat{h}_k s_k,\ \sigma_N^2(1+\kappa(1-\omega))\right).$$

The ability to distinguish between the two hypotheses is only through the difference in the means, and therefore it is critical that $\widehat{h}_k \neq 0$, i.e., $\omega > 0$. When the SNR is adequate, i.e., $\kappa \gg \frac{1}{1-\omega}$ (i.e., when the estimation error dominates, $E\widetilde{\sigma}^2 \gg \sigma_N^2$), the statistics become

$$y_k | \widehat{h}_k, s_k \ \sim \ \mathcal{CN}\left(\sqrt{E}\,\widehat{h}_k s_k,\ E\sigma_h^2(1-\omega)\right),$$

Increasing κ scales the variance and power in the mean equally, and so for large SNR κ, i.e., $\kappa \gg \frac{1}{1-\omega}$, performance saturates.

[1] Henceforth, we will use OOK(p_θ) to denote the binary alphabet with $p = p_\theta$, $A = 1/\sqrt{p_\theta}$, and $B = 0$.

4.2. Cutoff Rate for OOK

When no CSI is available at the receiver ($\omega = 0$), it has been shown that the capacity-optimal input distribution at low SNR is OOK [1]. Also, it was shown that, restricted to binary distributions, OOK is capacity optimal at all SNR. Here, we find that OOK modulation also maximizes the cutoff rate (equivalently, (2)) for all κ when $\omega = 0$. Since OOK(p) is optimal when $\omega = 0$, it remains only to determine the rate-maximizing transmission probability[2] p^*. Setting $A^2 = \frac{1}{p}$ (from the energy constraint), $B = 0$ and $\omega = 0$ in (2), p^* is given by

$$p^* = \min_{0<p<1} p(1-p) \left[\frac{\sqrt{1+\kappa\frac{1}{p}}}{1+\kappa\frac{1}{2p}} - 1 \right]. \tag{4}$$

Solving (4) yields p^* explicitly (as the relevant root of a fourth-order polynomial), and thus provides an easy characterization of the trade-off between the power of the non-zero mass point and its probability of transmission versus SNR. At low SNR, the probability of transmission is found to be

$$p^* \ = \ \frac{\tau^2 - 2\tau + 4}{6\tau}\,\kappa, \quad \text{where } \tau \triangleq \sqrt[3]{19 + 3\sqrt{33}}. \tag{5}$$

Compared to [1], equations (4) and (5) show that the cutoff rate gives a tractable way to characterize the optimal-binary input as a function of SNR.

Returning to the case of partial CSI, the OOK cutoff rate for arbitrary ω is

$$R_{o,K} = -\log_2 \left\{ 1 + 2p(1-p) \left[\frac{\sqrt{1+\kappa(1-\omega)\frac{1}{p}}}{1+\kappa\,(2-w)\,\frac{1}{4p}} - 1 \right] \right\}. \tag{6}$$

Analytic maximization of (6) over p leads to a high-order polynomial that has no explicit solution as a function of κ and ω. However, it can be verified that as $\kappa \to \infty$, $p^* \to 1/2$, and that as $\kappa \to 0, p^* \to 0$. Perhaps contrary to intuition, p^* is found to be non-monotonic as a function of ω at low SNR. Indeed, a second-order Taylor series expansion of (6) about $\kappa = 0$ reveals that

$$p^* = \frac{\sqrt{\kappa}}{2}\sqrt{\frac{-2 + 6\omega - 3\omega^2}{w}},$$

for $\omega > \omega^*$, which is decreasing for $\omega \in (\sqrt{2/3}, 1)$.[3]

Note that as κ increases, the optimal OOK amplitude A^* decreases (since $A^2 = \frac{1}{p}$). This trend was shown in [1] for the capacity metric and for no CSI ($w = 0$). From the

[2] By transmission probability, we mean the probability that the symbol A is transmitted.

[3] A third-order Taylor expansion yields an expression for p^* that is valid for all ω; it is omitted here for brevity.

figure, we see that when $\omega > 0$ this general trend is still true, and that for fixed κ, the optimal amplitude A^* is a decreasing function of ω; i.e., for poor CSI, the signalling is peaky. We see that for moderate to large values of κ, letting $p = 1/2$ is a reasonable approximation to p^*. Using $p = 1/2$, the cutoff rate becomes

$$R_{o,K} = -\log_2 \left\{ \frac{1}{2} + \frac{1}{2} \left[\frac{\sqrt{1 + 2\kappa(1-\omega)}}{1 + \kappa\left(1 - \frac{w}{2}\right)} \right] \right\}. \quad (7)$$

In Figure 2, we plot the cutoff rate for both OOK(p^*) and OOK($1/2$). Even at low SNR, the difference between the two OOK curves is seen to be small. OOK offers a significant advantage over BPSK for achieving high transmission rates. Unlike BPSK, the OOK cutoff rate saturates to 1 at high SNR for any CSI quality ω, and this gain is significant at moderate-to-large SNR. Also the OOK cutoff rate is non-zero when no CSI is available.

To understand this behavior, consider OOK($1/2$), and note that the statistics of y_k under the two hypotheses are:

$$y_k|\widehat{h}_k, s_k \ \sim \mathcal{CN}\left(\sqrt{E}\,\widehat{h}_k s_k,\ \sigma_N^2(1 + s_k^2\,\kappa(1-\omega)\right).$$

The distance between the means is obviously reduced compared to that for BPSK, however the variance terms are now distinct. We expect that if the difference in the variance terms is large enough (i.e., if κ is large enough), then OOK(1/2) will be able to outperform BPSK despite the decreased separation between means. Conversely, for small κ (when the variance terms are nearly identical), we expect BPSK to outperform OOK(1/2). Secondly, note that for no CSI ($\omega = 0$), the hypotheses become:

$$y_k|\widehat{h}_k, s_k \ \sim\ \mathcal{CN}\left(0,\ \sigma_N^2(1 + s_k^2\,\kappa\right),$$

and so, unlike BPSK, information transmission is possible under no CSI, particularly for large SNR κ.

From the preceding discussion, we expect that OOK will be optimal at large κ, and that BPSK will be optimal at small κ. What is the SNR at which one should switch from BPSK to OOK? We provide an answer in the next section.

4.3. Comparing BPSK and OOK

The results presented here give an *analytic basis* for an adaptive modulation scheme in which the transmitter can select between OOK($1/2$) and BPSK based only on the SNR κ and CSI quality ω available at the receiver. The transitional SNR $\bar{\kappa}$ is found by equating (3) and (7). This yields a third-order polynomial. Retaining the relevant root yields $\bar{\kappa} = f(\omega)$, where

$$f(\omega) = \left[\frac{(a+b)^{1/3} + (a-b)^{1/3} - 2\left(4 - 10\omega + 3\omega^2\right)}{3(2-\omega)^2(1-\omega)} \right],$$

with the definitions

$$a \triangleq 81\omega^6 - 468\omega^5 + 828\omega^4 - 640\omega^3 + 624\omega^2 - 192\omega + 64,$$

$$b \triangleq 6\sqrt{3}(\omega-2)^2 w^2 \sqrt{61\omega^4 - 208\omega^3 + 168\omega^2 - 64\omega + 16}.$$

The function $f(\omega)$ depends on the CSI quality, and is shown by the dashed line in Figure 3. At the end points, our result is as expected: $f(0) = 0$, implying that OOK is superior to BPSK at any SNR when no CSI is available, and $\lim_{\omega\to 1} f(\omega) = \infty$, implying that BPSK is superior to OOK when full CSI is available.

The solid line in Figure 2 depicts the threshold curve for OOK(p^*). To find this region we equate (3) and (6)(using the p^* from (4)), and solve for the transitional κ numerically. As expected, optimizing over p results in OOK being superior to BPSK over a wider range of SNR for any fixed ω. Interestingly, we find that there is a threshold value of CSI below which BPSK is not useful. A low SNR analysis once again reveals this threshold value of CSI to be $\omega^* = 1 - 1/\sqrt{3}$.[4]

4.4. Analysis of Adaptive Modulation Schemes

The impact of both adaptive modulation schemes on the cutoff rate is shown in Figure 4. As upper and lower benchmarks, we also show the cutoff rates for optimal binary signaling, and for pure-BPSK and pure-OOK, when $\kappa = 0$ dB. All curves have been normalized by the cutoff rate for optimal binary signaling. As expected, the BPSK/OOK($\frac{1}{2}$) scheme simply traces out the best of the BPSK and OOK cutoff rates. Notice that pure-BPSK performs arbitrarily poorly for small ω, while pure-OOK is suboptimal by up to 60-percent at high SNR. In contrast, *the OOK(p)/BPSK scheme performs nearly as well as optimal binary signaling over the entire range of* ω. To understand this interesting fact, we partition the (κ, ω) plane into three regions in Figure 5: (a) the region where BPSK is optimal, (b) the region where OOK(p^*) is optimal, and (c) the region where neither is optimal. Over most of the (κ, ω) plane, we see that either BPSK or OOK(p^*) is indeed optimal. In conclusion, we see that adaptive modulation ensures high-rate transmission at all values of (κ, ω).

5. ENERGY-OPTIMAL MODULATION

In Section 4, we studied the modulation that results in the largest cutoff rate for a fixed SNR. However, many networks need only operate at a specified and fixed rate. In these networks, the goal is to use the modulation that is most energy efficient, and we consider this problem next.

[4]This reoccurrence of ω^* is to be expected. Earlier in this section we found that, among all binary inputs, only OOK(p^*) or BPSK is optimal at low SNR.

5.1. Equiprobable OOK

It is well known that when full receiver CSI is available, using OOK$(1/2)$ instead of BPSK incurs a 3 dB energy penalty for all R_o [11]. Here, we examine this penalty under partial CSI, and show that the maximum penalty is 4 dB. We also show that this penalty decreases for smaller values of ω and R_o, eventually becoming a "gain".

Define the energy penalty incurred for using BPSK in place of OOK$(1/2)$ to be

$$\gamma \triangleq \frac{\kappa_{\text{BPSK}}}{\kappa_{\text{OOK}(1/2)}}; \quad \gamma_{\text{dB}} \triangleq 10\log_{10}\gamma,$$

so that $\gamma_{\text{dB}} < 0$ indicates a penalty for using OOK$(1/2)$, while $\gamma_{\text{dB}} > 0$ indicates a penalty for using BPSK (therefore, in our notation, the well-known result states that $\gamma_{\text{dB}} = -3$ for full receiver CSI, and for all R_o). Substitution yields

$$\gamma = \frac{(1-\frac{\omega}{2})^2(\omega-(1+\lambda))^{-1}(1+\lambda)\lambda^2}{(1-\omega)-\lambda^2(1-\frac{\omega}{2})+\sqrt{\lambda^2(-1+\frac{\omega}{2})(1-\frac{3}{2}\omega)+(1-\omega)^2}},$$

for $R_o < -\log_2(1-\omega/2)$, which we plot in Figure 6. The following remarks are in order:

R10. For small R_o, the 3 dB penalty for using OOK$(1/2)$ persists, even under partial CSI. It is easy to show that $\gamma_{\text{dB}} \to -3$ as $R_o \to 0$, for *all* ω.

R11. For non-vanishing R_o however, the 3 dB penalty rule no longer holds. It is clear from the figure, that there exists a (R_o, ω) region where $\gamma_{\text{dB}} \leq -3$). It can be shown that (proofs have been omitted due to space limitations):(a) the maximum energy penalty occurs for some $\omega \in (0.8, 1)$, which is an increasing function of R_o (b) the penalty is greater than 3 dB if and only if

$$\omega \in \left(\frac{2}{3}, 1\right) \text{ and } R_o \leq -\log_2\frac{1-\sqrt{-3+6\omega-2\omega^2}}{2(1-\omega)},$$

and (c) the largest penalty occurs for $R_o = 1^-$ and $\omega = 1^-$, and has an infimum of $\gamma_{\text{dB,min}} = 10\log_{10}(2/5) \approx -4$ dB. Therefore, *there is at most an additional* 1 *dB increase in the penalty due to imperfect receiver CSI.*

R12. Conversely, OOK$(1/2)$ may actually provide an energy "gain" for some values of R_o and ω. Setting $\gamma = 1$, we find the (R_o, ω) curve for which these two constellations are equally energy efficient to be given by the valid root of the fourth order polynomial,

$$\lambda^4 - 2\lambda^3 + \frac{\omega^2-8\omega+4}{\omega^2}\lambda^2 + 8\left(\frac{1-\omega}{\omega}\right)^2\lambda + 4\left(\frac{1-\omega}{\omega}\right)^2.$$

Based on the results in **R10**-**R12**, we can partition the (R_o, ω) plane as shown in Figure 7.

5.2. OOK with variable probability

From [5], we know that when full receiver CSI is available, the 3 dB penalty for using OOK$(1/2)$ (in place of BPSK) is partially recovered by using OOK$(p^\star)$ instead, where $p^\star$ is the energy-minimizing transmission probability. It was shown that a full recovery is possible as $R_o \to 0$. However, in the last section, we showed that OOK$(1/2)$ may provide either penalty or a gain relative to BPSK, when only imperfect CSI is available. Therefore, we will not discuss how much we are able to "recover" by using OOK$(p^\star)$ in place of BPSK. Rather, we will discuss how much we are able to gain by using OOK$(p^\star)$ instead of OOK$(1/2)$.

The transmission probability $p^\star$ that minimizes the energy required to attain R_o, for a given ω, is given by

$$p^\star = \arg\min_{0\leq p\leq 1/2} \kappa_{\text{OOK}(p)} \tag{8}$$

and, clearly, the resulting required energy is given by $\kappa_{\text{OOK}(p^\star)}$. In general, (8) does not yield a closed form expression (CFE) for $p^\star$. However, it is easy to verify that as $R_o \to 0, p^\star \to 0$ and that as $R_o \to 1, p^\star \to 1/2$. Additionally, when full CSI is available ($\omega = 1$), (8) yields the CFE

$$p^\star = \sqrt{\frac{1-2^{-R_o}}{2}}. \tag{9}$$

When no CSI is available, and the target R_o is small ($R_o \to 0$), (8) yields

$$p^\star = \alpha(1-2^{-R_o}), \alpha \triangleq \left[\frac{7+\sqrt[3]{199-3\sqrt{33}}+\sqrt[3]{199+3\sqrt{33}}}{6}\right],$$

which implies that the transmission probability grows logarithmically in R_o.

Next, we define χ to be the energy penalty for using OOK$(1/2)$ in place of OOK$(p^\star)$,

$$\chi \triangleq \frac{\kappa_{\text{OOK}(1/2)}}{\kappa_{\text{OOK}(p^\star)}}, \quad \chi_{\text{dB}} \triangleq 10\log_{10}\chi\,.$$

Note $\chi_{\text{dB}} \geq 0$ since OOK$(p^\star)$ will always be at least as energy efficient as OOK$(1/2)$. We plot χ_{dB} in Figure 8 for small R_o, and make the following remarks:

R13. *For small rates ($R_o \to 0$).* It was seen in the previous section that the 3 dB OOK$(1/2)$ penalty persists for all values of ω. Note that with OOK$(p^\star)$ there is a 3 dB gain for (approximately) $\omega \in (0.4, 1)$. Therefore, the well-known 3 dB penalty is recovered with OOK$(p^\star)$, not just for full CSI as shown in [5], but also for moderate to large values of CSI. In addition, for $\omega \in (0.0, 0.4)$, OOK$(p^\star)$ "more than recovers" the 3 dB penalty imposed by OOK$(1/2)$. That is, OOK$(p^\star)$ is *more energy-efficient than BPSK*. As $\omega \to 0$, the energy savings grows arbitrarily large.

R14. *For large rates ($R_o \to 1$).* As $R_o \to 1$, the gain of OOK$(p^\star)$ relative to OOK$(1/2)$ approaches 0 dB for all ω.

This is because as $R_o \to 1$, $p^\star \to 1/2$ (see the discussion after Equation (8)), making the two inputs equivalent. In particular, the maximum penalty for using OOK$(1/2)$ in place of BPSK was seen to be 4 dB, which occurs as $(R_o \to 1, \omega \to 1)$. Therefore, *this* 4 *dB penalty persists, even when OOK(*$p^\star$*) is used in place of OOK(*$1/2$*).*

6. DISCUSSION

We have derived signal design strategies for wireless communications that describe how to best allocate each of the major system resources: power, bandwidth, and modulation, when only imperfect channel state information is available at the receiver. We have assumed that the transmitter has knowledge of the SNR and Doppler spread only, and that it requires *no explicit feedback of the instantaneous channel state.* Such designs will be useful in tactical communications scenarios and sensor networks, where feedback may be limited, and where energy efficient signalling is critical from many perspectives (such as interference, LPD/LPI, transceiver complexity, network lifetime).

7. REFERENCES

[1] I. Abou-Faycal, M. Trott, S. Shamai. "The Capacity of Discrete-Time Memoryless Rayleigh-Fading Channels," *IEEE Trans. Info. Theory*, 47(4), 1290-1301, May 2001.

[2] I.F. Akyildiz, S. Weilian, Y. Sankarasubramaniam, E. Cayirci, "A Survey on Sensor Networks," *IEEE Comm. Magazine*, 40(8), 102-113, August 2002.

[3] J. Baltersee, G. Fock, H. Meyr, "An Information Theoretic Foundation of Synchronized Detection," *IEEE Trans. Comm.*, Vol. 49, No. 12, pp.2115-2123, December 2001.

[4] E. Biglieri, J. Proakis, and S. Shamai, "Fading Channels: Information-Theoretic and Communications Aspects", *IEEE Trans. Info. Theory*, 44(6), 2619-2692, Oct 1998.

[5] J.M. Geist, "The Cutoff Rate for On-Off Keying", *IEEE Trans. Comm.*, Aug. 1991.

[6] A.O. Hero and T.L. Marzetta, "Cutoff rate and signal design for the quasi-static Rayleigh fading space-time channel", *IEEE Trans. Info. Theory*, Vol. 47, No. 6, pp.2400-2416, September 2001.

[7] S. Jamali, and T. Le-Ngoc, *Coded-Modulation Techniques for Fading Channels.* Kluwer Academic Publishers, 1994.

[8] J. Massey, "Coding and Moulation in Digital Communications," In *Proc. 1974 Int. Zurich Seminar., Digital Communication*, March 1974.

[9] S. Misra, A. Swami, and L. Tong, "Rate-Optimal Binary Inputs with Partial CSI," *IEEE Trans. Comm.*, Submitted August 2004. Also see [10].

[10] S. Misra, A. Swami, and L. Tong, "Optimal Training for Correlated Fading Channels," ARL Technical Report TR-3193, April 2004.

[11] J. Proakis, *Digital Communications*, McGraw Hill, 4ed.

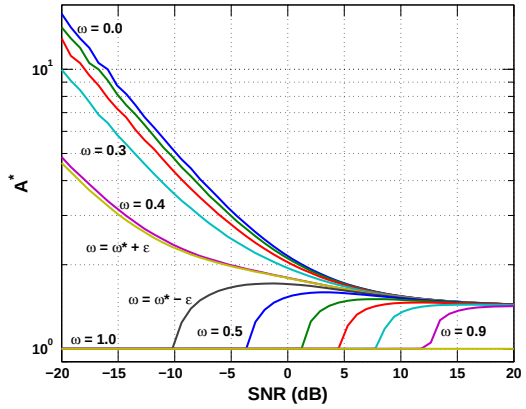

(a) A^* vs. SNR $\mathcal{K}$ for several values of ω

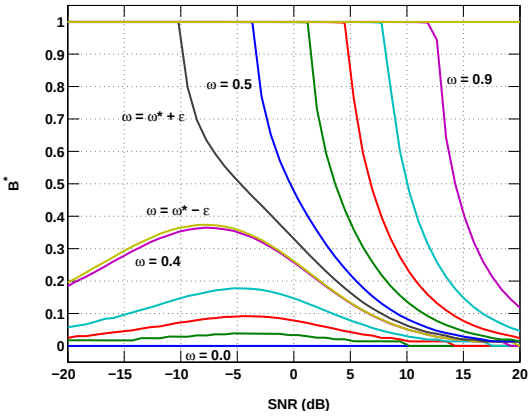

(b) B^* vs. SNR $\mathcal{K}$ for several values of ω

Fig. 1. The optimal binary input (A^*, B^*) versus SNR κ for several values of ω. The quantity $\epsilon \triangleq 0.01$ is used to illustrate behavior around the $\omega = \omega^*$ breakpoint.

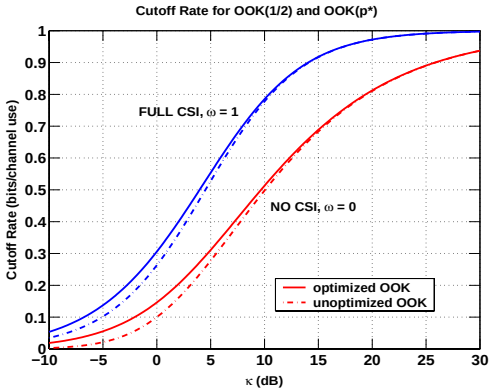

Fig. 2. The OOK cutoff rate $R_{o,K}$ vs. SNR κ (dB), for different values of the CSI quality ω, when: (a) $p = 1/2$, and (b) $p \in (0, 1/2)$ is optimized.

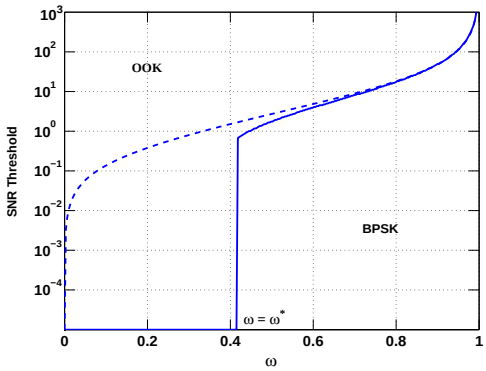

Fig. 3. The transitional SNR $\bar{\kappa} = f(\omega)$, above which OOK is optimal and below which BPSK is optimal, for: (a) OOK$(1/2)$ and (b) OOK(p^*) (solid line).

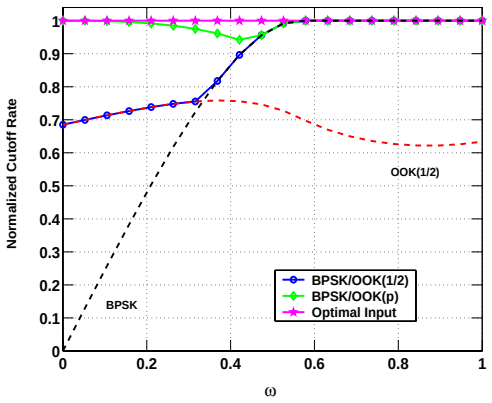

Fig. 4. The normalized cutoff rate for a single data channel versus the CSI quality ω, and for five different binary transmission strategies with $\kappa = 0$ dB. The CSI quality is treated as a free parameter; no underlying estimation scheme is assumed.

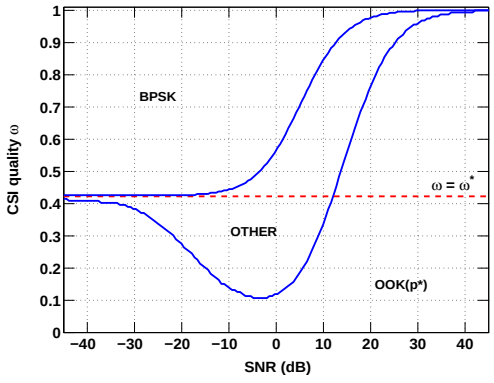

Fig. 5. A partitioning of the $(\mathrm{SNR}(\kappa), \mathrm{CSI}(\omega))$ plane into the following three regions: (a) where BPSK is optimal, (b) where OOK(p^*) is optimal, and (c) where some other binary input is optimal.

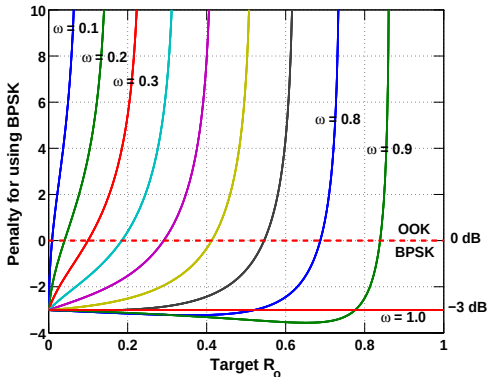

Fig. 6. Energy penalty γ_{dB} vs. target cutoff rate R_o for several values of CSI quality ω. A negative value of γ_{dB} indicates that BPSK is more energy efficient than OOK$(1/2)$.

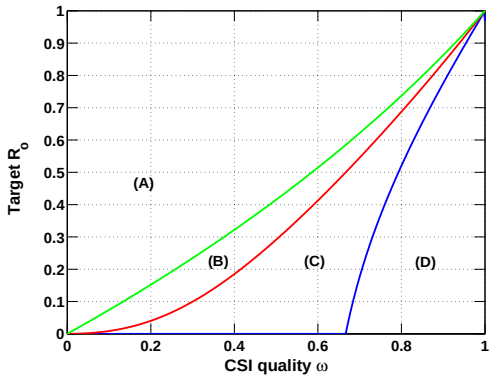

Fig. 7. A partitioning of the (R_o, ω) plane into regions where the energy penalty for using BPSK in place of OOK$(1/2)$ is: (A) "∞" dB, (B) between 0 dB and 3 dB, (C) between -3 dB and 0 dB, and (D) less than -3 dB. Note that the maximum penalty is ≈ 4 dB, and occurs for $R_o = 1^-$ and $\omega = 1^-$.

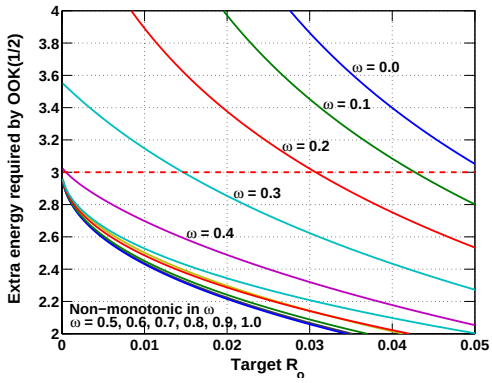

Fig. 8. A plot of χ_{dB}, the energy-penalty for using OOK$(1/2)$ in place of OOK(p^*), for various values of the target cutoff rate R_o (R_o small) and CSI quality ω. For larger values of ω, χ_{dB} is seen to be non-monotonic in ω.